

Supporting information for

**Highly dispersed Cu₂O quantum dot (about 2 nm) constructed by
simple functional group anchoring strategy: Boosts 72 times
photocatalytic water splitting ability**

Jindou Hu¹, Xiangjun Shen¹, Anjie Liu, Zhenjiang Lu, Jing Xie, Aize Hao, Xinhui Jiang,

Jiangfeng Wang, Yali Cao*

State Key Laboratory of Chemistry and Utilization of Carbon Based Energy
Resources; College of Chemistry, Xinjiang University, Urumqi, 830017, Xinjiang, PR
China.

*Corresponding author. Tel: +86-991-8583083; Fax: +86-991-8588883.

E-mail: caoyali523@163.com, hujindou@xju.edu.cn

Characterization

The morphology, sizes of the obtained photocatalysts and the energy dispersive spectrometry (EDS) data were measured using a Hitachi S-4800 scanning electron microscopy (SEM) at 5 kV. The high-resolution transmission electron microscopy (HRTEM) images and elemental mapping images of the as-synthesized materials were recorded on a JEOL JEM-2010F transmission electron microscope at 200 kV. X-ray diffraction (XRD) was performed on a Bruker D8 X-ray diffractometer with a Cu-K α radiation in the 2 θ range of 10-80°. Fourier transform infrared spectra (FT-IR) were recorded on a Bruker VERTEX 70 IR spectrometer using KBr pellets. The X-ray photoelectron spectroscopy (XPS) was measured on a Thermo Fisher Scientific

ESCALAB 250Xi photoelectron spectrometer. Ultraviolet-visible (UV-vis) absorption spectra of the as-obtained photocatalysts were measured using a Hitachi U-3010 spectrophotometer during 250-800 nm at room temperature. An electron spin resonance spectrometer (Evisa JES-FA300) was used to obtain the electron paramagnetic resonance (EPR) spectroscopy. CHI 760E electrochemical instrument was used to perform the Mott-Schottky curves with a three-electrode quartz cells (Counter electrode: Pt wire; Reference electrode: Ag/AgCl; Working electrode: photocatalysts coated ITO glass). The 300 W Xe lamp of Beijing China Education Aulight Co., Ltd. was used as the light source. A Vis REF standard visibility mirror was used with a light source wavelength of 350-780 nm. The photoluminescence spectra (PL) were obtained on a Hitachi F-4500 fluorescence spectrophotometer (excitation wavelength: 250 nm). Gas chromatograph (GC 7920, conductivity detector (TCD), N₂ carrier gas).

Photocatalytic hydrogen evolution measurement

Photocatalytic hydrogen evolution (PHE) experiments were carried out on an online photocatalytic hydrogen evolution system (CEL-SPH2NP, Beijing China Education Aulight Co., Ltd.). The quartz reaction kettle is used as a container, and the closed gas circulation system and gas extraction system are connected at the interface by coating vacuum grease. 0.1 g of photocatalyst was dispersed in 100 mL of aqueous solution containing 25 mL of methanol and dispersed uniformly under sonication. methanol was chosen as the cavity sacrificial agent and a 300W Xe lamp was used as the light source. Before the reaction, the reactor is degassed several times to remove air from the reactor. Volatile hydrogen was determined by online gas chromatography (GC 7920, conductance detector (TCD), N₂ carrier gas), and the precipitated gas was analyzed and detected every 1 h.

Photocatalytic stability test

Three times (15h) photocatalytic hydrogen evolution experiments were carried out on the photocatalytic hydrogen evolution system, including a 5-hour cycle. After the end of one cycle, the reactor was taken down and stood for a period of time, and then vacuumized again to continue the next cycle hydrogen production experiment.

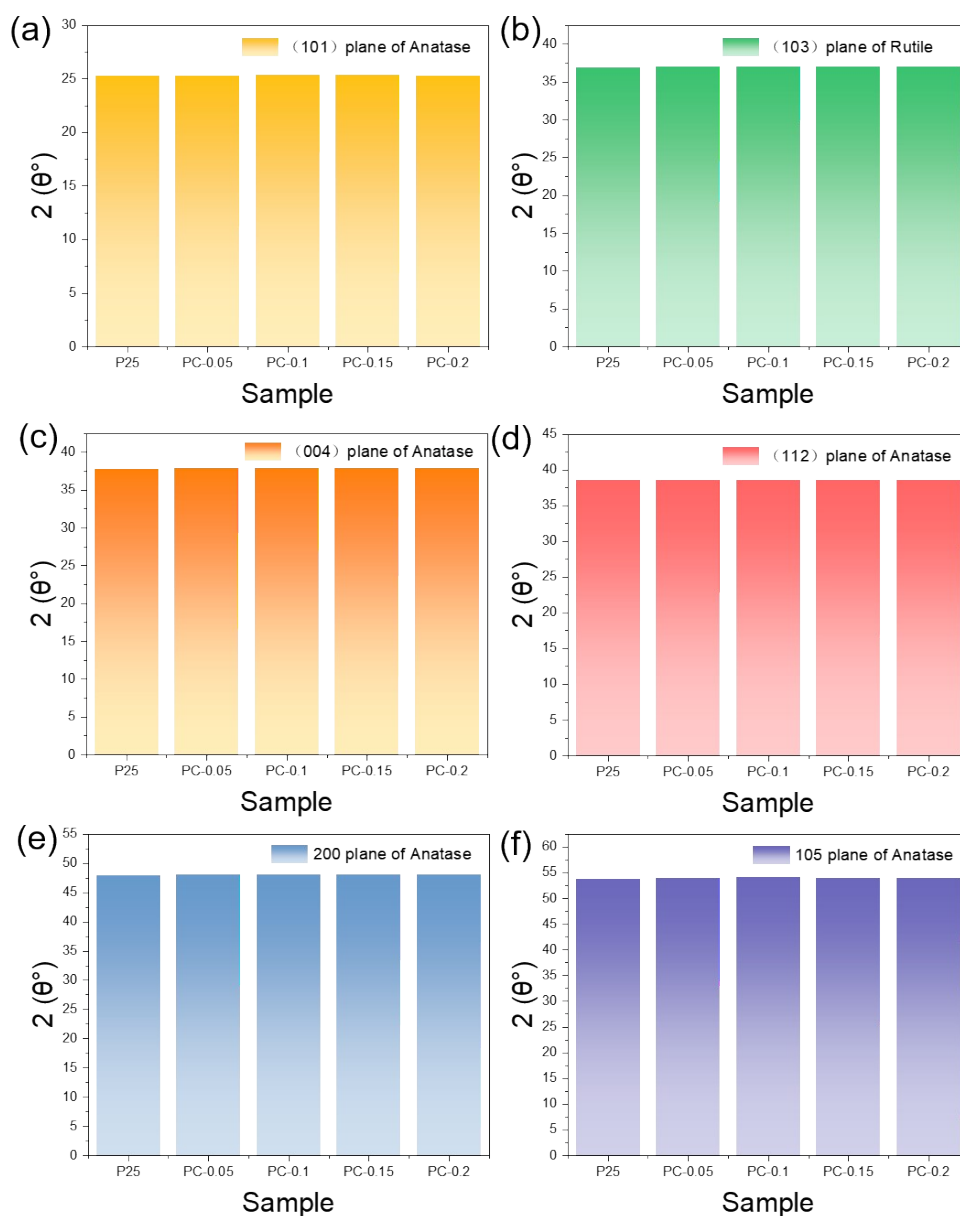


Fig. S1. The peak position of each sample in XRD: a. (101) plane of anatase; b. (103) plane of Rutile; c. (112) plane of anatase; d. (004) plane of anatase

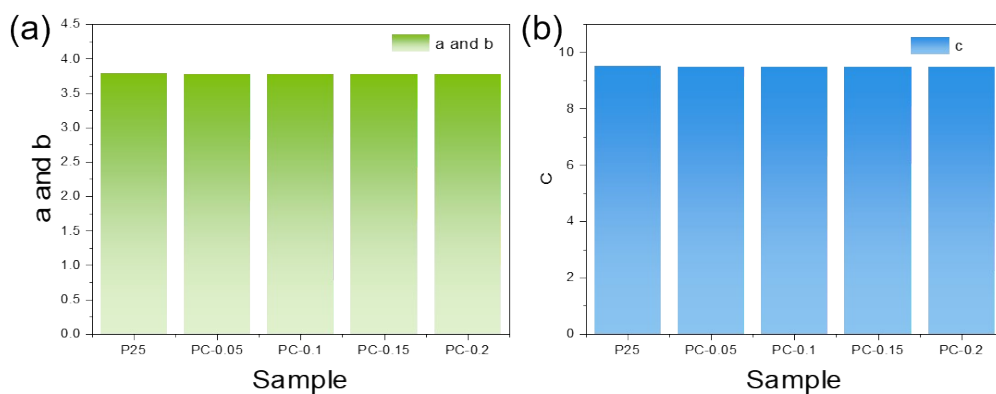


Fig. S2. The calculated lattice constant of each sample from XRD.

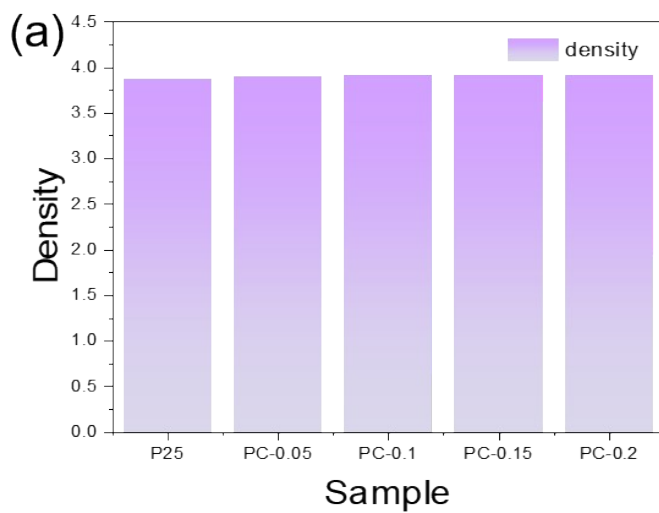


Fig. S3. The calculated lattice density of each sample from XRD.

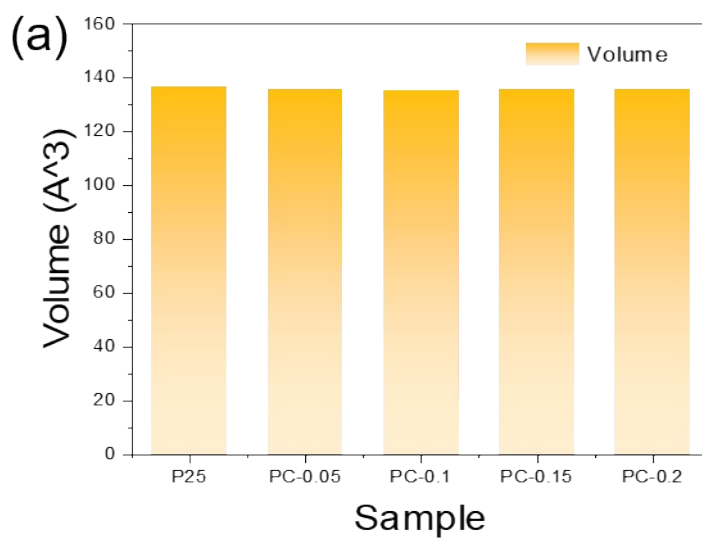


Fig. S4. The calculated lattice volume of each sample from XRD.

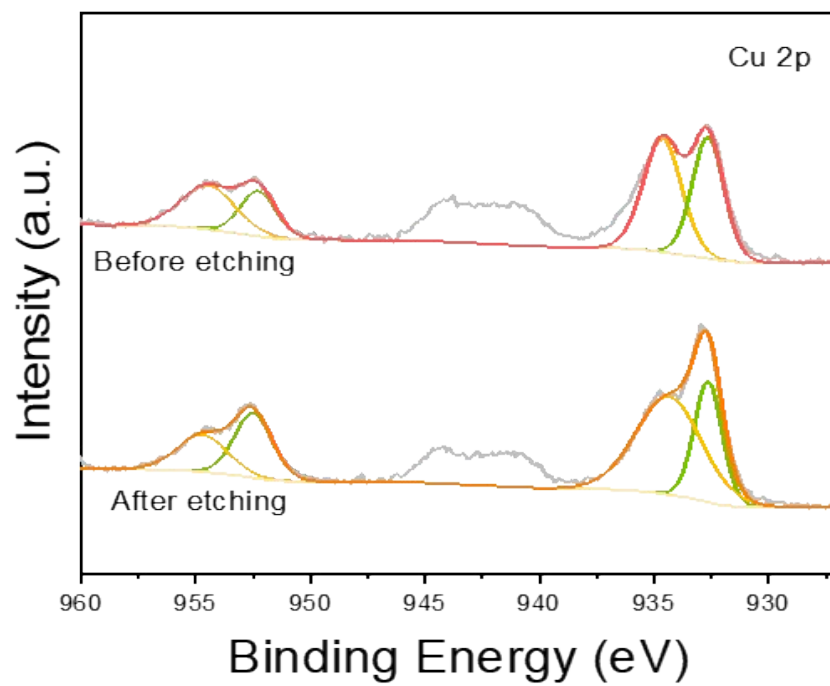


Fig. S5. Comparison of high-resolution XPS spectra of Cu before and after etching.

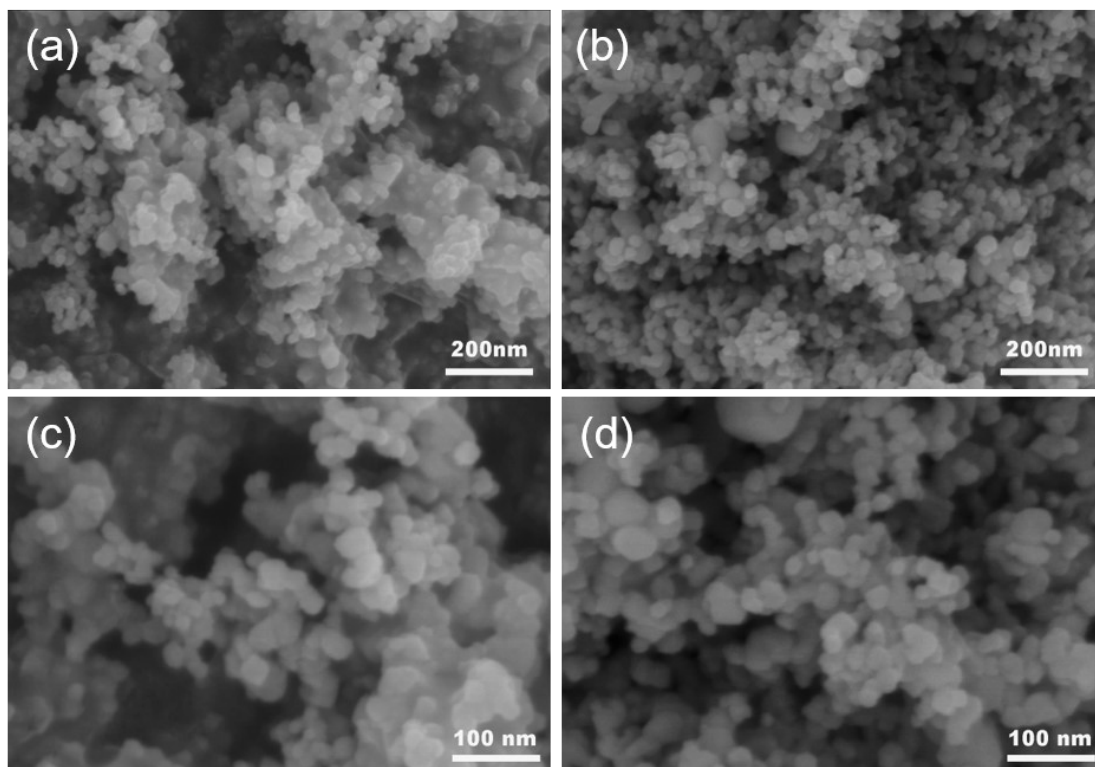


Fig. S6. SEM images of P25 10w (a),20w (c) and PC-0.1 10w (b),20w (d)

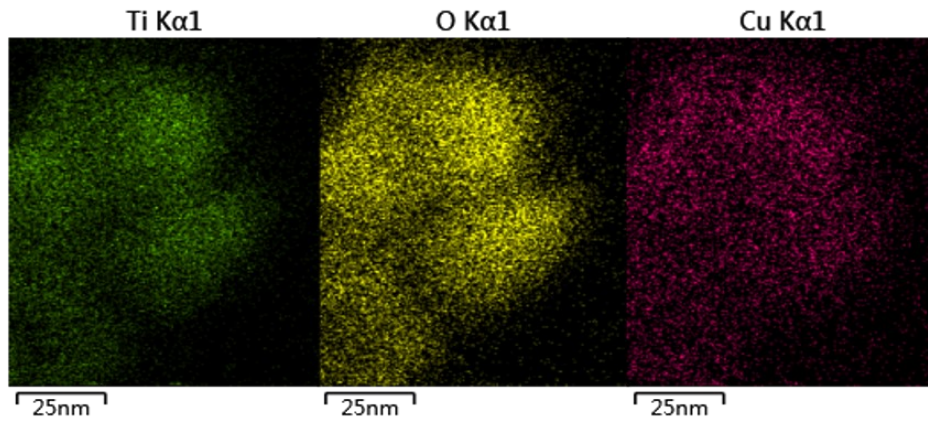


Fig. S7. Elemental mapping of PC-0.1 for Ti, O, Cu.

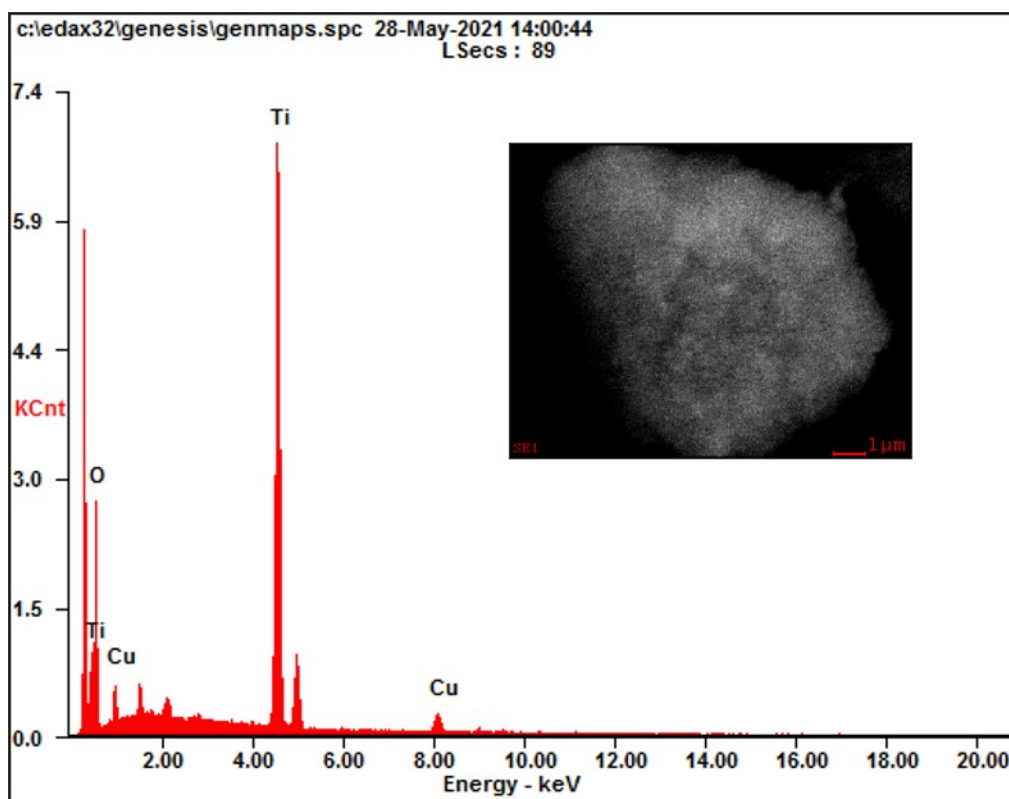


Fig. S8. Element contents of PC-0.1

Table S1. Element contents of PC-0.1

Element	Wt%	At%
OK	44.41	71.08
TiK	49.53	26.48
CuK	06.06	02.44
Matrix	Correction	ZAF

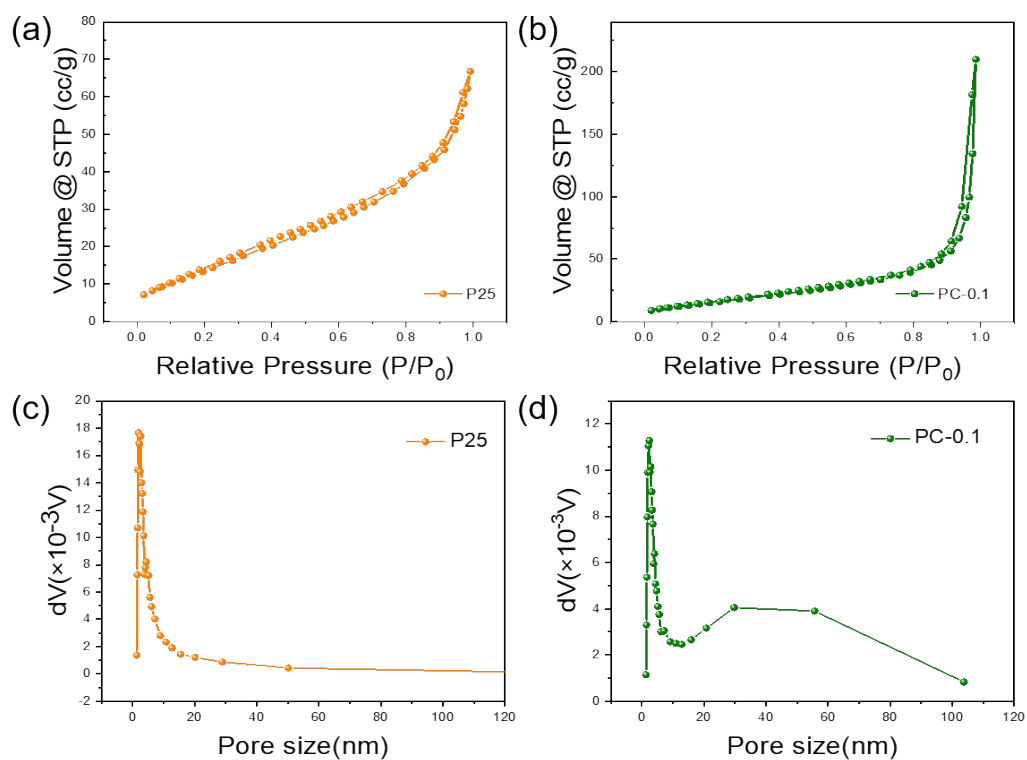


Fig. S9. pore size distributions of P25 (a) and PC-0.1 (b), N₂ adsorption–desorption isotherms of P25 (c) and PC-0.1 (d).

Table S2. The surface area, pore volume and pore diameter of P25 and P-ANL-3

Sample	Surface Area (m ² /g)	Pore Volume (cc/g)	Pore Diameter (nm)
P25	82.395	0.114	1.194
PC-0.1	70.140	0.330	2.574

Table S3. Comparisons of the photocatalytic H₂ evolution of the catalysts prepared in the present work with the recently reported TiO₂-based catalysts.

Photocatalyst	Light Source	H ₂ evolution rate/($\mu\text{mol}\cdot\text{g}^{-1}\cdot\text{h}^{-1}$)	Reference
This Work	300 W Xe lamp	14911	-
TiO ₂ /rGO	3 W-LED (365 nm, 80 mW cm ⁻²)	103.82	[1]
Cu-TiO ₂	UV (450 W Hg)	8470	[2]
Ni/TiO ₂	UV (450 W Hg)	3390	[3]
Pt/TiO ₂	AM 1.5 G solar simulator	11200	[4]
Cu/TiO ₂	UV (450 W Hg)	8470	[3]
Cu/S-TiO ₂	500 W Xe lamp with UV cut off filter	7500	[5]
Pt/Ga-TiO ₂	150 W Xe lamp	5722	[6]
Rh/Nb-TiO ₂	300 W Xe lamp	7850	[7]
TiO ₂ -His	Xe lamp	216.3	[8]

References

- [1] Cao Y, Wang P, Fan J, Yu H, Covalently functionalized graphene by thiourea for enhancing H₂-evolution performance of TiO₂ photocatalyst, *Ceram. Int.* 47 (2021) 654-661.
- [2] Kumaravel V, Mathew S, Bartlett J, Pillai S C, Photocatalytic hydrogen production using metal doped TiO₂: A review of recent advances, *Appl.Catal.B Environ.* 244 (2019) 1021-1064.
- [3] Montoya A T, Gillan E G, Enhanced photocatalytic hydrogen evolution from transition-metal surface-modified TiO₂, *ACS Omega.* 3 (2018) 2947-2955.
- [4] Banerjee B, Amoli V, Maurya A, Sinha A K, Bhaumik A, Green synthesis of Pt-doped TiO₂ nanocrystals with exposed (001) facets and mesoscopic void space for photo-splitting of water under solar irradiation, *Nanoscale.* 7 (2015) 10504-10512.
- [5] Zhang W, Wang S, Li J, Yang X, Photocatalytic hydrogen production from methanol aqueous solution under visible-light using Cu/S-TiO₂ prepared by

- electroless plating method, *Catal. Commun.* 59 (2015) 189-194.
- [6] Luo S, Nguyen-Phan T D, Vovchok D, Waluyo I, Palomino R M, Gamalski A D, Barrio L, Xu W, Polyansky D E, Rodriguez J A, Senanayake S D, Enhanced, robust light-driven H₂ generation by gallium-doped titania nanoparticles, *Phys. Chem. Chem. Phys.* 20 (2018) 2104-2112.
- [7] Huang J, Li G, Zhou Z, Jiang Y, Hu Q, Xue C, Guo W, Efficient photocatalytic hydrogen production over Rh and Nb codoped TiO₂ nanorods, *Chem. Eng. J.* 337 (2018) 282-289.
- [8] Han X, Ma H, Wang C, Li Y, Enhanced photocatalytic hydrogen production by loading histidine on TiO₂, *J. Phys. Energy* 3(2020) 014001-014010.